REPORT DOCUMENTATION PAGE

Form Approved
OMB No. 0704-0188

1. REPORT DATE *(DD-MM-YYYY)* 01-11-2005	REPRINT	
4. TITLE AND SUBTITLE Atmospheric Considerations in Engagement-Level Simulations of Tactical High-Energy Laser Systems		**5a. CONTRACT NUMBER** **5b. GRANT NUMBER** **5c. PROGRAM ELEMENT NUMBER** 61102F
6. AUTHOR(S) G.Y. Jumper, J.R. Roadcap, S.C. Adair*, G.P. Seeley* and G. Fairley*		**5d. PROJECT NUMBER** 2304 **5e. TASK NUMBER** 0T **5f. WORK UNIT NUMBER** A1
7. PERFORMING ORGANIZATION NAME(S) AND ADDRESS(ES) Air Force Research Laboratory/VSBY 29 Randolph Road Hanscom AFB MA 01731-3010		**8. PERFORMING ORGANIZATION REPORT NUMBER** AFRL-VS-HA-TR-2005-1159
9. SPONSORING / MONITORING AGENCY NAME(S) AND ADDRESS(ES)		**10. SPONSOR/MONITOR'S ACRONYM(S)** **11. SPONSOR/MONITOR'S REPORT NUMBER(S)**

12. DISTRIBUTION / AVAILABILITY STATEMENT
Approved for Public Release; Distribution Unlimited.

*RADEX, Lexington, MA

13. SUPPLEMENTARY NOTES
REPRINTED FROM: JOURNAL OF DIRECTED ENERGY, Vol 1, pp 183-201, Fall 2005.

14. ABSTRACT

The atmosphere can have a tremendous impact on tactical high-energy laser (HEL) systems. The variable nature of the atmosphere can produce highly variable performance. System designers need accurate environmental models to optimize the design of these systems. This paper reviews the atmospheric impact of various atmospheric phenomena on laser performance and the measurement and modeling efforts of the Air Force Research Laboratory. Two of these phenomena, optical turbulence and cloud obscuration, have been included in an engagement-level model, DEEST (Directed Energy Environmental Simulation Tool), to determine the optical performance of a tactical laser system. DEEST is described, and various aspects of the model are discussed for the benefit of those who will be modeling tactical HEL systems.

15. SUBJECT TERMS
Optical Turbulence
Atmospheric transmission
Atmospheric effects simulation
High energy laser systems

16. SECURITY CLASSIFICATION OF:			**17. LIMITATION OF ABSTRACT**	**18. NUMBER OF PAGES**	**19a. NAME OF RESPONSIBLE PERSON**
a. REPORT		**c. THIS PAGE**			George Jumper
UNCLAS	UNCLAS	UNCLAS	SAR		**19b. TELEPHONE NUMBER** *(include area code)* 781-377-3148

Journal of Directed Energy, **1**, Fall 2005, 183–201

Atmospheric Considerations in Engagement-Level Simulations of Tactical High-Energy Laser Systems

George Y. Jumper* and John R. Roadcap

Air Force Research Laboratory, AFRL/VSBY, 29 Randolph Road, Hanscom Air Force Base, Massachusetts 01731-3010

and

Sara C. Adair, Guy P. Seeley, and Gerard Fairley

Radex, Inc., 131 Hartwell Avenue, Lexington, Massachusetts 02421-3126

The atmosphere can have a tremendous impact on tactical high-energy laser (HEL) systems. The variable nature of the atmosphere can produce highly variable performance. System designers need accurate environmental models to optimize the design of these systems. This paper reviews the atmospheric impact of various atmospheric phenomena on laser performance and the measurement and modeling efforts of the Air Force Research Laboratory. Two of these phenomena, optical turbulence and cloud obscuration, have been included in an engagement-level model, DEEST (Directed Energy Environmental Simulation Tool), to determine the optical performance of a tactical laser system. DEEST is described, and various aspects of the model are discussed for the benefit of those who will be modeling tactical HEL systems.

KEYWORDS: Atmospheric effects simulation, Atmospheric transmission, Optical turbulence

Nomenclature

A_j	weighting function for the water specie j (l, liquid water; i, ice; r, rain; s, snow) [nondimensional (nd)]
C	weighted sum of water specie densities (kg/m^3)
C_j	mixing ratio of water specie i, weight of water specie to weight of dry air (nd)
C_P	integrated density of weighted water species along beam path (kg/m^2)
C_n^2	structure constant of index of refraction (m$^{-2/3}$), a measure of optical turbulence
f_c	Greenwood frequency (Hz)
k	wave number of propagated radiation (1/m)
L_T	total path length of transmission (m)
$\bar{r}$	radius vectors from center of Earth to points along beam path (m)
r_0	Fried's coherence length (m)
s	transmission path distance (m)

Received May 4, 2004; revision received March 21, 2005.

*Corresponding author; e-mail: george.jumper@hanscom.af.mil.

V_n	relative wind speed normal to beam path (m/s)
α_P	elevation angle at a point P along the beam path (rad)
λ	wavelength of propagated radiation (m)
σ_I^2	normalized intensity variance or scintillation index (nd)
σ_χ^2	Rytov variance (nd)
θ_E	interior angle from vector, $\bar{r}_i$ pointing to beam source to vector, r at an arbitrary point along beam path (rad)
θ_0	isoplanatic angle (rad)
τ	atmospheric transmittance (nd)

1. Introduction

The atmosphere contains a number of effects that can significantly impact the performance of directed energy systems. Optical turbulence, clouds, dust, fog, and marine aerosols diminish the amount of energy that arrives at a target. Optical turbulence, which is characterized by a fluctuating index of refraction, causes beam scintillation, wandering, and broadening. Clouds, fog, dust, and other aerosols play a critical role in scattering and absorption. System designers must consider these effects to determine optimum wavelengths, required system power, optical requirements, and overall effectiveness. Quantifying all these effects is highly complex, yet mission planners for fielded systems will require calculations in a timely manner to use high-energy laser (HEL) assets in an effective manner. One significant atmospheric effect that is not included in this paper is the distortion of the atmosphere caused by the laser weapon system.

Capturing the variations in length scales and physical processes that are typically involved in directed energy scenarios requires a collection of models. Different military scenarios call for different models or combinations of models from the collection. For example, predicting atmospheric conditions for a ground-based or ship-based laser system is heavily dependent on surface and boundary layer considerations, whereas predicting conditions in the path from a high-altitude airborne system is more strongly affected by jet stream and mountain-induced gravity wave behavior. Therefore, choosing appropriate models requires understanding the phenomena that are important for a given scenario and knowledge of available models.

To fully realize all the desired optical performance capabilities of the directed energy optical turbulence models, the most relevant models must be adapted and selectively implemented to describe an entire region of interest, despite the variety of atmospheric regimes it may contain. Furthermore, model results that quantify local path conditions must be combined to indicate optical parameter quantities for specific paths of interest. Such a tool would perform the model calculations and, in addition, find the relevant path-dependent quantities. The user interface must accommodate end users who are not familiar with the specific models but require information about specific paths of interest. Since future research might introduce new models or improvements to existing models, any system developed must be adaptable enough to allow for improvements that take advantage of such progress. To be useful the tool must use standardized protocols and input data.

2. Atmospheric Phenomena

Clearly the atmospheric phenomena of interest for a laser weapon system will be strongly dependent on details of the intended use. Altitude of laser and target will be a predominant

Table 1. Notional list of the relative importance of some atmospheric phenomena on possible laser system missions. $H_2O(v)$ is water vapor absorption, as separated from the absorption by other gaseous molecules. L is for low impact, M is for moderate, and H is for high. If more than one letter is present, then the impact can vary over the range, depending on conditions. TMD stands for theater missile defense. Propagation problems due to distortions of airflow around laser weapons are not included

Atmospheric Phenomena \ Missions	ABL TMD	Air to Air	Air to Ground	Ground to Air	Ship Defense
C_n^2	H	M	M	M	M
Clouds	M	H	H	H	H
Aerosols	L	L	H/M	H/M	H/M
H2O(v)	L	L	M	M	H
Other Molec Absorb	L	L	H/L	H/L	H/L
Blooming	L	L	M/H	M/H	H
Path Refraction	L	L	M	M	H

factor, while speed and geographic location will also be important. For discussion purposes, Table 1 is a notional listing of the relative impacts of some atmospheric phenomena on possible laser missions. Individual laser systems and scenario details could change the ranking. The chart depicts the fact that for high-altitude, theater-scale scenarios the most important atmospheric effect is optical turbulence (labeled C_n^2). Optical turbulence is the result of turbulent mixing of pockets of air with different indices of refraction that cause the laser beam irradiance to scintillate, spread, or otherwise distort. For altitudes below the tropopause, clouds can become the major impact to laser propagation. Also, as either laser or target gets nearer to the ground, aerosols such as smoke, dust, and haze become important. The amount of water vapor that can be carried by the atmosphere increases with decreasing altitude and increasing air temperature. At lower altitudes, water vapor absorption becomes the most important consideration for laser wavelength selection, especially at lower altitudes over bodies of water. The absorption of laser radiation by water vapor becomes the predominant mechanism for converting laser radiation into local heating of the atmosphere. If there is low relative speed of the beam through the air, the air can become heated enough to cause changes in the index of refraction, which distorts the beam. The result is called "thermal

blooming," and it can be a dominant factor for fixed or slowly moving lasers or targets. At lower altitudes, beam bending due to refraction gradients can be very important, especially over water.[5]

3. Suggested Modeling Approach

There are many ways to evaluate the effectiveness of candidate systems. While each atmospheric effect has a range of possible impacts, simple calculations using the best, worst, and average conditions are often misleading. Near-worst-case conditions of every parameter are never seen in a real atmosphere. In the case of atmospheric optical turbulence, a worst case of, say, the 2-sigma extreme at every altitude results in a condition that is much worse than any single measured vertical profile. In reality, the index of refraction structure constant C_n^2 can be very high at certain locations, say, in the high shear regions around a jet stream or in the atmospheric boundary layer, but optical turbulence conditions at other locations along the beam path may be low to moderate.

To account for the variability of the atmosphere, we have settled on an evaluation approach based on statistical analysis of a mission scenario through a series of representative atmospheric conditions. Scenario definition is extremely important. The geographic location, the altitudes of laser and target, the velocity of each, the season, and even the time of day can affect the outcome.

The scenario will dictate the complexity of the atmospheric models. With the long quasi-horizontal paths associated with theater missile defense (TMD) missions, a full three-dimensional model of the atmosphere is desirable. For shorter ranges, azimuthal symmetry can become a reasonable assumption and a one-dimensional "profile" of atmospheric conditions can suffice. When range dictates that the curvature of the Earth can affect the results, then the single profile is applied to the calculation as an "onion-skin" model in which the parameters are constant on a spherical surface. For shorter paths, a flat-Earth layered approach in which the parameters are constant on the plane is appropriate. For the shortest-distance scenarios of nearly coaltitude weapon and target, constant atmospheric parameters can be applied along the path. For scenarios in which one-dimensional models will suffice, we have used actual atmospheric profiles in either layered or onion-skin models. For cases that require a full three-dimensional atmosphere, we have been using parameters derived from mesoscale meteorological forecast models. It can be argued that certain scenarios might dictate that a two-dimensional or slab-symmetric model be applied. A case in point would be a fairly long-distance shot over both land and water; however, we have never used this approach.

4. Modeling Using One-Dimensional Atmospheric Profiles

The Air Force Research Laboratory (AFRL), Hanscom Research Site, is the custodian of a number of high-resolution atmospheric profiles of normal radiosonde data, i.e., temperature, pressure, humidity, and wind speed and direction, in addition to the optical turbulence parameter, C_n^2, from ground level to 30 km. These data include locations in the continental United States (CONUS) as well as regions of potential conflict. Collectively, the data are known as "thermosonde" data since thermosonde is the name of the instrument that was used to measure optical turbulence. The thermosonde is attached to a meteorological radiosonde, which rises through the atmosphere by means of a large weather balloon and sends down the turbulence data to the radiosonde ground station as "spare channel" data.

For a good example of the use of thermosonde data to determine the impact of the atmosphere on tactical HEL systems, see Ref. 19. That paper describes the use of the onion-skin model to analyze many of the effects of importance to lasers. Given the placement of laser system and target, the initial analysis is to properly define the laser path through the atmosphere. The spherical Earth path equation is shown in Sec. 7. Since the profile of mean atmospheric density is known, the refracted path can be computed as described in Ref. 19, if it is a concern. Given altitude as a function of beam path distance, a variety of performance parameters can be determined.

Many of the effects are shown in two-dimensional contour plots of the effect as a function of laser to target surface distance and altitude. For example, Fig. 1 shows the mean, spherical wave Rytov variance σ_χ^2 and path transmittance τ for an air-to-ground (or ground-to-air) scenario.

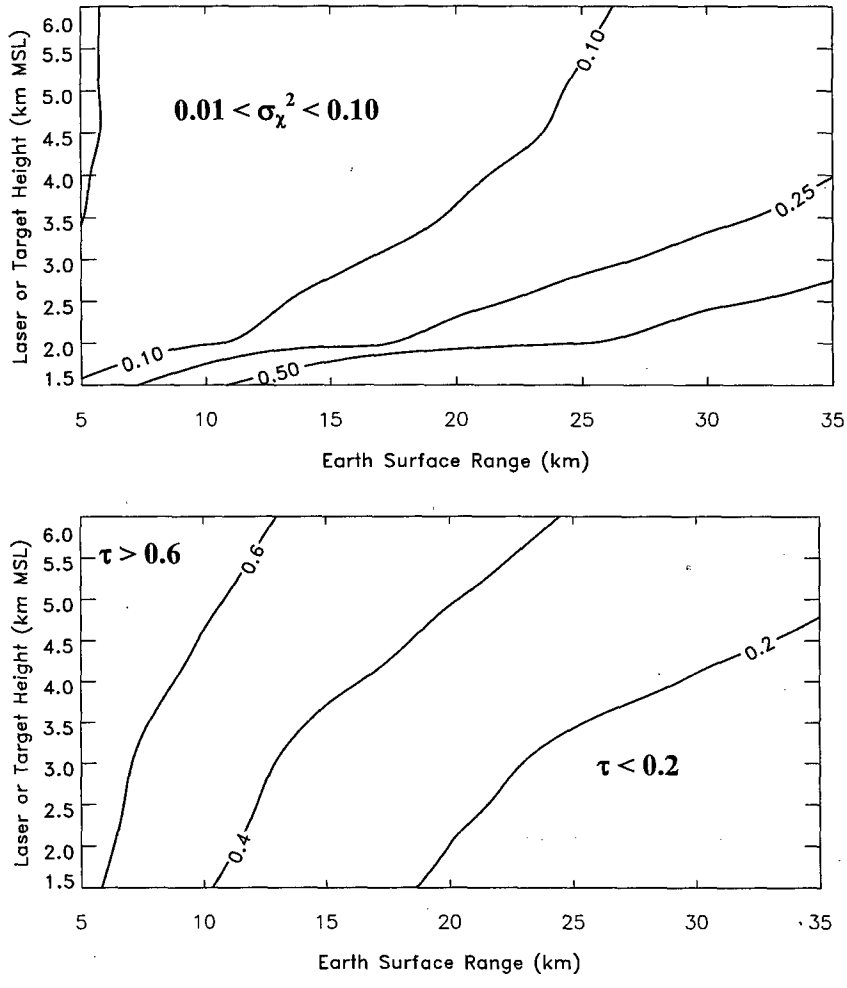

Fig. 1. Contour plots of mean Rytov variance and path transmittance for air-to-ground slant paths as a function of laser/target height and Earth surface distance. Wavelength is 1.315 μm.

The important optical turbulence performance parameters, Fried coherence length r_0, isoplanatic angle θ_0, and Rytov variance σ_χ^2, are all functions of C_n^2 and the geometry of the problem, as shown in Sec. 7.2. Two other parameters, Greenwood frequency f_c and Tyler frequency f_T, use the additional input of the velocity of the air relative to the laser beam, which requires the velocities (speed and direction) of laser, target, and wind.

The profiles can also be used to deduce other effects. A technique to estimate the absorption and scatter from aerosols is described in Ref. 19, along with the calculation of molecular absorption, by using values from the HITRAN database described in Ref. 22. HITRAN is periodically upgraded; potential users should visit the HITRAN internet site.[13]

Roadcap et al.[19] also describe the use of the profiles with HITRAN absorption values to estimate the effect of thermal blooming on the laser beam by calculation of the atmospheric distortion index. The distortion index calculations are described more fully in Ref. 20.

5. Three-Dimensional Models

What has been more difficult is trying to generate three-dimensional models of the atmospheric phenomena that affect directed energy systems. Except for some very short distances, it is extremely difficult to obtain three-dimensional measurements of atmospheric properties, especially C_n^2. Beginning in 1999, whenever a full three-dimensional description of atmosphere impacts is required (four dimensions if time is included), AFRL researchers have used the output of research-grade and operational mesoscale meteorological models. The current AFRL research capability[23] uses the output of a modified version of MM5, which is the mesoscale model currently used by operational Air Force weather organizations.[24] The C_n^2 level is estimated by a postprocessing technique using the Dewan model.[4] The technique was also adapted for the use of the astronomical community in Hawaii.[3] Walters and Miller at the Naval Postgraduate School have also been forecasting C_n^2 (Ref. 17) with the Navy Coupled Ocean/Atmosphere Mesoscale Prediction System (COAMPS), which uses a different turbulence model.

5.1. DEEST

The AFRL three-dimensional modeling research approach discussed above has been incorporated into the Directed Energy Environmental Simulation Tool (DEEST).[1] To date, the DEEST model is limited to optical turbulence and cloud obscuration effects. These effects are computed by using operational meteorological data that are readily available. The original DEEST version used only MM5 model data and only data over the CONUS region, but it is capable of using any other operational data in World Meteorological Organization Gridded Binary (GRIB) format. DEEST was designed for future incorporation of new operational models and new user interface elements as needed to expand applicability. The latest version of DEEST can also ingest one-dimensional atmospheric profiles such as routine weather balloon data and apply them in onion-skin fashion for shorter engagements. While originally constructed as a research-grade decision aid for the TMD mission, it became clear that it had other modeling and simulation value.

DEEST is an optical atmospheric effects simulation tool that selects and applies models from its collection according to user-specified Euclidean paths of interest. DEEST ingests input data, performs preliminary calculations, requests and accepts user input, implements selected models, postprocesses model results, and interactively displays model results. To

date, DEEST can be considered only an "atmospheric subroutine" of larger laser system analysis models. Only certain optical performance parameters are computed by DEEST, and it is left to the user, perhaps with a higher-level simulation, to determine the final effect of these parameters on the effect of the target on the weapon.

Collectively, the models contained in DEEST require an extensive amount of atmospheric data. Operational Air Force Weather Agency (AFWA) data have been used to drive the DEEST models. Data produced by the Penn State–National Center for Atmospheric Research (NCAR) MM5 were found to be suitable.[6–8,11,12,28–31] MM5 is a mesoscale, nonhydrostatic, compressible model, which predicts temperature, winds, humidity, clouds, and precipitation. MM5 is operationally run at AFWA four times per day with forecast data output every 3 h out to 72 h in the future for several regions around the globe. While DEEST is designed to ingest any input grid size including the research-grade, finer-scale model mentioned earlier, it usually uses the operational CONUS region results with a grid spacing of 15 km horizontally and nonuniform vertical spacing. Since optical turbulence length scales are on the order of tens of meters thick and kilometers wide, the length scales are clearly well below the resolution of a 15-km grid, or the resolution of most mesoscale meteorological models. Consequently, optical turbulence must be computed by using subgrid-scale parameterization or other modeling tools.

If DEEST is to be used for an upcoming mission, MM5 output as run in its typical mode is requested from AFWA for the region of interest, and it is stored in one of the standard output formats. The operational forecast data are downloaded to the DEEST workstation, and the available dates and times are listed for user selection. If the forecast output is not selected ahead of time, MM5 can be run for a time and place of interest by using archived initialization information.

DEEST does preliminary calculations to compute quantities that are needed for the models. For example, the AFWA data are delivered in sigma levels, which are terrain-following, pressure-based levels that define the MM5 vertical coordinate. The data are transformed from sigma levels to height levels by DEEST. DEEST then computes optical turbulence and cloud quantities for the entire domain of data ingested. Optical turbulence, or C_n^2, is calculated by using either one or several models as appropriate to the atmospheric regime. Cloud indicators for the domain are found by taking a weighted average of the cloud quantities from MM5.

As a consequence of using the Dewan model, DEEST must identify the tropopause height for the purposes of selecting between troposphere-appropriate and stratosphere-appropriate coefficients for the C_n^2 computations. In DEEST, the geometric heights and the temperature field are used to calculate the temperature lapse rates. The tropopause is defined as the lowest vertical layer that is more than 1 km thick and has a vertical temperature gradient that is greater than -2.8°C per km. The more standard definition, which uses a threshold of -2.0°C per km, was considered too high given the smoothness of model data. The restriction of using a layer more than 1 km thick typically does not change the outcome but is included to ensure that a layer is large enough to give a meaningful representation of the tropopause. Although multiple tropopauses are possible in the atmosphere, DEEST computes only the lowest tropopause altitude that meets the criteria.

DEEST uses a graphical user interface (GUI) to request and accept user input, such as the date and the path of interest. Path-dependent turbulence quantities are calculated as needed from an extensive list, including Greenwood frequency, Rytov variance, and coherence length. DEEST results are interactively displayed both numerically and graphically. For example, cloud images can be superimposed on C_n^2 results, and horizontal or vertical cross

sections of turbulence and cloud effects on performance data can be displayed for different sections according to user request.

The remainder of this paper describes the various components of DEEST, leading up to how DEEST users would simulate and analyze laser system scenarios. This includes information on data setup, preliminary calculations, DEEST modeling, techniques used in DEEST, cloud representation, and cloud path obscuration.

6. Modeling

6.1. Optical turbulence modeling

DEEST addresses the impacts of optical turbulence and clouds on optical performance parameters. Optical turbulence, or random fluctuations in the index of refraction, is commonly quantified in terms of the refractive index structure constant C_n^2. This structure constant can be defined in terms of the related structure function and the power law it satisfies.[2] In general, turbulence throughout the free atmosphere occurs in layers that are on the order of kilometers in lateral extent and tens of meters thick in regions of shear instabilities. Models are required to predict the relatively small-scale turbulence events based on the larger-scale mesoscale model data available.

Some of the optical turbulence model inputs are wavelength dependent. To preserve the flexibility to transform wavelength from a fixed value to a user-specified value, model components that pertain to other wavelengths are incorporated into DEEST. However, at this time the ability to specify wavelength is not present in the DEEST interface. The DEEST model uses the wavelength of 1.315 μm, which is in the near-IR region of the electromagnetic spectrum. In the future, DEEST can be expanded to allow the DEEST interface user to modify wavelength values.

Different C_n^2 models are included in DEEST to account for the different atmospheric regimes and to accommodate data availability. Five models are used to span atmospheric regimes as determined by geometric height or pressure level and land–water status. The models and their associated atmospheric regimes are listed in Table 2. The common practice of setting the surface layer height to one-tenth of the planetary boundary layer (PBL) height[14] is used in DEEST. The PBL height is readily available as it is one of the MM5

Table 2. DEEST C_n^2 models and their regions of applicability

Region	C_n^2 Model	
Above MM5 model top	CLEAR 1	
Above PBL and below MM5 model top	Dewan	
Within PBL and above surface layer	Kaimal (Unstable) or Dewan (Stable)	
Surface layer	Over land: Tunick	Over water: Frederickson and Davidson

variables ingested by DEEST. Surface layer calculations are subdivided into land and water layers, according to MM5 land-use values. The model of Tunick[18,26,27] and the model of Fredrickson et al.[9] are used for land and water surface layers, respectively. The *Tunick* model uses surface layer temperature gradients and the Monin–Obukhov similarity theory to compute turbulence length scales and the optical turbulence structure parameter C_n^2; different equations apply for stable and unstable conditions. Stability is computed from the vertical temperature gradient. Unstable conditions are common for humid atmospheres in the daytime. The *Fredrickson and Davidson* model[9] also uses the Monin–Obukhov similarity theory and is based on mean environmental buoy measurements, such as air–sea temperature differences. Above the surface layer and within the PBL, the model depends on the atmospheric stability. If the PBL is unstable, the Kaimal et al.[16] model is used. The *Kaimal* model intakes the precomputed surface layer C_n^2 value as a reference value and calculates other C_n^2 values as a function of altitude. The C_n^2 drop-off rate differs in the surface layer, mixed layer, and entrainment zone, as computed from atmospheric conditions. Within a stable PBL and above the PBL up to the maximum MM5 altitude, the model of Dewan et al.[4] is used. The *Dewan* model is a Tatarski-based[25] model that uses empirical relationships and first-order turbulence closures to compute inertial range turbulence length scales and C_n^2 values, respectively. Above the MM5 model top, where no forecast data are available, the CLEAR1 statistical model[2] is used. The CLEAR1 model is a function of altitude alone.

6.2. Cloud and precipitation representation

Clouds are quantified in terms of the cloud values provided by the MM5 input data and are determined to be either opaque or clear to a given path according to the algorithm described below. Clouds and precipitation are quantified in DEEST by using mixing ratios of the four water species contained in the MM5 output. The four mixing ratios are cloud liquid, cloud ice, rain, and snow, denoted here by C_l, C_i, C_r, and C_s, respectively. These are combined to obtain a single value for each point in the atmospheric data grid to represent the amount of cloud and/or precipitation at that point. The resulting water specie values are integrated along the path of interest and compared to a threshold to determine whether integrated cloud conditions are severe enough to obscure laser propagation. The weighting used to combine mixing ratios is discussed below, and the path-dependent calculations pertaining to clouds are explained in Sec. 7.2.

Each mixing ratio indicates mass of that water specie per unit mass of dry air.[21] DEEST uses a linear combination of these to evaluate the total amount of water substance at any point due to all types. For the purposes of cloud obscuration, it is more relevant to consider the density of water species in the path (i.e., cloud liquid water content, rain water content, cloud ice water content, and snow water content). The specie density is obtained by multiplying the local mixing ratio by the local dry air density ρ_d. The result of this operation and the linear combination gives the total weighted density of water at a point as

$$C = \rho_d (A_l C_l + A_i C_i + A_r C_r + A_s C_s)$$

where A_l, A_i, A_r, and A_s are the user-specified weighting coefficients for liquid, ice, rain, and snow mixing ratios, respectively. The default values for these coefficients, established by visual comparisons to satellite imagery, are as follows: $A_l = 1.0$, $A_i = 7.0$, $A_r = 1.0$, and $A_s = 1.0$. These values can be replaced by user-specified values.

7. Calculation Techiniques

7.1. Path ray tracing

A ray tracing algorithm is used by locating the points along a Euclidean straight path between the user-specified laser system and target locations. A coordinate system is introduced to simplify the task of specifying a straight line between these two points. Though the new coordinate system is natural for defining straight lines, it is not convenient for referencing points in the Earth's atmosphere. Atmospheric quantities are stored by DEEST on the nonuniform MM5-based grid. Thus, much of the computation involved in the ray tracing algorithm is to transform path and atmospheric information between coordinate systems. All ray tracing in DEEST is performed as in a vacuum, that is, without beam bending by refraction, which is a second-order effect compared to the MM5 resolution.

The coordinate system used to define a straight path is a rectangular system that is fixed with respect to the Earth. The path is fixed with respect to the coordinate system and therefore the Earth. The path endpoints are specified by the user in terms of latitudes, longitudes, and heights above the earth (lat/lon/z). These two locations are transformed to the rectangular coordinates used to define the path, called the ray tracing coordinates. The path is described numerically by nodes that are equally spaced in the ray tracing coordinates. For each node along the path, its location is first transformed to the lat/lon/z system and then to the nonuniform grid on which atmospheric data are stored by DEEST. Latitude and longitude are available on an indexed grid since they are variables in the MM5 output. Thus a lat/lon position is described in DEEST by the nearest i, j location within the grid. Then atmospheric data pertaining to the node's location are accessed and used to calculate various path-dependent quantities, such as optical turbulence integrals.

The ray tracing algorithm processes each node along the path in succession until one of two things happens: the arrival at the ray endpoint or encountering a situation that prevents arrival at the ray endpoint. The stopping conditions reflect beam extinction by cloud obscuration or intersection of the ground, or an attempt to calculate beyond the extent of the C_n^2 data (altitude >30 km or outside the region of MM5 data). If one of these conditions occurs, then DEEST stops the calculation and identifies the problem.

7.2. Integration of optical turbulence parameters

The influence of optical turbulence on laser propagation along a path can be characterized in terms of turbulence parameters. All of the turbulence parameters in DEEST are path integrals of C_n^2 weighted by path metrics and, in one case, air speed. The specific integrals are given below.

The optical performance parameter calculations used in DEEST are all based on weak scattering theory for fully developed turbulence with a Kolmogorov distribution.[2] In all cases DEEST performs the path integrals discretely by using the nodes mentioned above. For all integrals except the Greenwood frequency,[10] the calculations can be done by directly applying the ray tracing to the precomputed C_n^2 values. The Greenwood frequency requires additional wind and vehicle velocity calculations, which are described later. The integrals are performed from the source of the radiation at 0 to the target at L_T, the total path length. Some of the quantities yield the same result if computed in the opposite direction; some do not. The spherical wave results are used for a point source within the atmosphere to a

target. The plane wave results apply to an exoatmospheric source, such as a star, that results in nearly plane waves entering the atmosphere.

The Rytov variance is used to compute the scintillation of the beam. It is a reasonable measure of the turbulence impact on weapon performance. The plane wave Rytov variance for a path from 0 to L_T is given by

$$\sigma_\chi^2 = 0.56k^{7/6}\int_0^{L_T} C_n^2(s)(L_T - s)^{5/6}ds,$$

where k is the wave number of the propagated radiation.† Spherical wave Rytov variance is

$$\sigma_\chi^2 = 0.56k^{7/6}\int_0^{L_T} C_n^2(s)\left[\frac{s(L_T - s)}{L_T}\right]^{5/6}ds.$$

The normalized intensity variance, sometimes called the scintillation index, is

$$\sigma_I^2 = \exp\left(4\sigma_\chi^2\right) - 1.$$

Coherence length, sometimes called Fried's coherence length, is the maximum effective optical diameter given the presence of turbulence. The plane wave coherence length (m) is

$$r_0 = 2.1\left[1.46k^2\int_0^{L_T} C_n^2(s)ds\right]^{-3/5},$$

The spherical wave coherence length (m) is

$$r_0 = 2.1\left[1.46k^2\int_0^{L_T} C_n^2(s)\left(\frac{s}{L_T}\right)^{5/3}ds\right]^{-3/5},$$

The isoplanatic angle (rad) is a measure of the coherence angle between an incoming beam from a target and an outgoing beam trying to hit the target. It is found by using

$$\theta_0 = \left[2.91k^2\int_0^{L_T} C_n^2(s)s^{5/3}ds\right]^{-3/5},$$

The Greenwood frequency (Hz), a measure of required adaptive optics frequency response, is

$$f_c = \left[0.102k^2\int_0^{L_T} C_n^2(s)(V_n(s))^{5/3}ds\right]^{3/5},$$

where V_n is a relative wind speed in the plane orthogonal to the path. This speed takes into account atmospheric winds and the speeds of the system and target. To compute this wind speed, the problem is decomposed into horizontal (tangent to the Earth's surface and perpendicular to the Earth radius vector) and vertical (perpendicular to the Earth's surface and parallel to the Earth radius vector) components at each point along the path (Fig. 2). All r vectors in Fig. 2 originate from the center of the Earth. DEEST uses the assumption that the laser aircraft motion is confined to the horizontal plane. The missile motion is assumed to be strictly vertical. Then, using MM5 horizontal and vertical wind speeds, at each point in the path, the relative wind speeds in the horizontal and vertical can be computed, then projected onto the plane perpendicular to the path, and finally combined to obtain V_n.

†$k = 2\pi/\lambda$, where λ is wavelength.

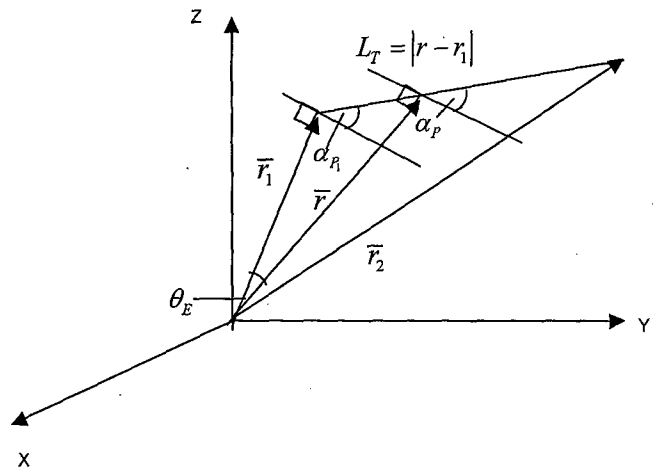

Fig. 2. Geometry of the ray between two locations designated by the vectors $\bar{r}_1$ and $\bar{r}_2$. The vector $\bar{r}$ points to an arbitrary computation point along the ray.

The radius vectors come from the center of the Earth, and the interior angle between the location of the laser at $\bar{r}_1$ and an arbitrary point on the ray defined by the vector $\bar{r}$ is defined by the equation

$$\theta_E = \left| \cos^{-1} \left| \frac{\bar{r} \bullet \bar{r}_1}{r_1 r} \right| \right|.$$

Figure 2 gives the basic geometry of all ray tracing used for calculation of all parameters. The initial elevation angle in Fig. 2 is α_{p_i}, so for any point along the ray, the elevation angle is $\alpha_p = \alpha_{p_i} + \theta_E$. The distance between vectors $\bar{r}$ and $\bar{r}_1$ is $\bar{L}_T| = |\bar{r} - \bar{r}_1|$. Use of the law of cosines on the triangle formed by r, r_1 and L_T gives

$$r^2 = r_1^2 + L_T^2 - 2 r_1 L_T \cos(90 + \alpha_{p_i}).$$

Solving this equation for α_{p_i} yields

$$\alpha_{p_i} = \sin^{-1} \frac{|r^2 - r_1^2 - L_T^2|}{2 r_1 L_T}.$$

Inserting this into the equation $\alpha_p = \alpha_{p_i} + \theta_E$ results in

$$\alpha_p = \sin^{-1} \frac{|r^2 - r_1^2 - L_T^2|}{2 r_1 L_T} + \theta_E.$$

7.3. Cloud obscuration along a path

The cloud content (kg/m^2) for a given path is found by integrating the local water content $C(s)$, defined in Sec. 6.2, along the path to obtain

$$C_p = \int_0^{L_T} C(s) ds,$$

where s is a path-following distance. This integral is approximated by a sum of local cloud content values along a path determined by the system and target locations, according to the ray tracing method presented in Sec. 7.2. If the value of C_p exceeds a user-specified threshold, then the path is considered opaque to transmission.

8. Using DEEST to Analyze a Laser System Scenario

DEEST provides the user with information about optical turbulence and clouds. The information is available in graphical output to assist in mission planning. In addition, DEEST provides numerical results for optical turbulence performance integrals shown in Sec. 7.2. In the main menu screen (not shown), the user specifies the time and date of the analysis and the target parameters. Given the position of a potential target, DEEST provides various tools to assist in positioning a laser system to ensure adequate performance in an engagement. The laser weapon positional planning screen is shown in Fig. 3. The user clicks on the background image to horizontally position the target watchbox and the laser system. To assist the user in positioning the weapon system, there are buttons on the screen for creating azimuthal views and vertical cross sections.

Generally, the first question for the planner is the azimuthal position of the laser system relative to the target. If the viewer selects the Create Azimuthal View button, a window displays a view similar to Fig. 4. The colors indicate the lowest spherical Rytov values

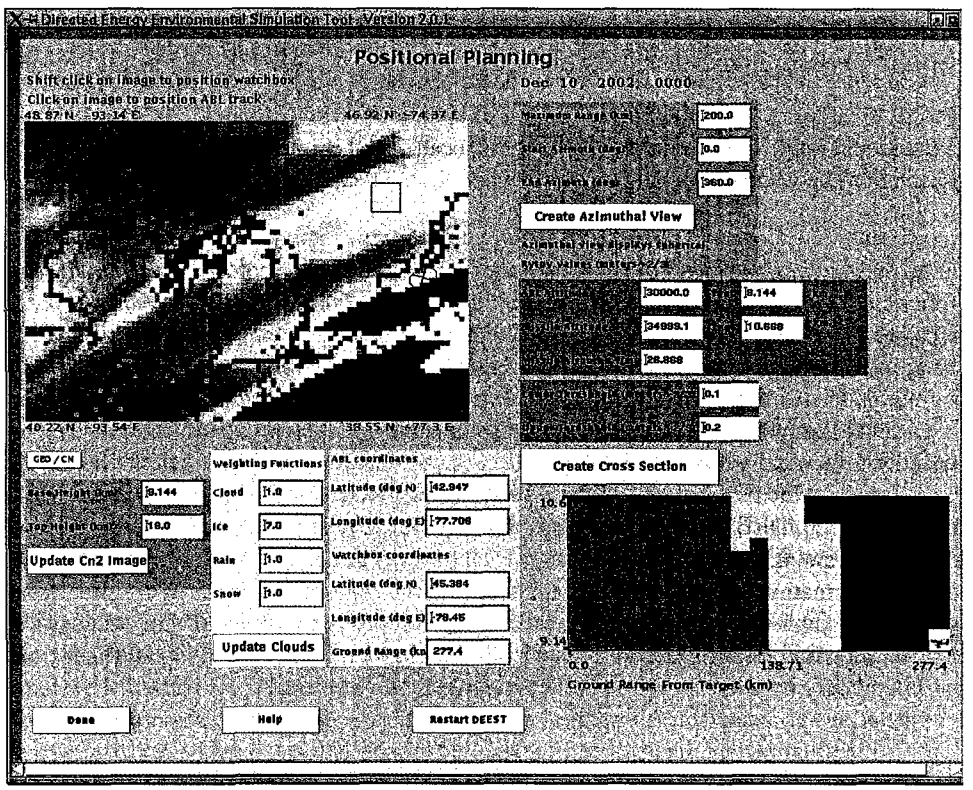

Fig. 3. DEEST positional planning screen.

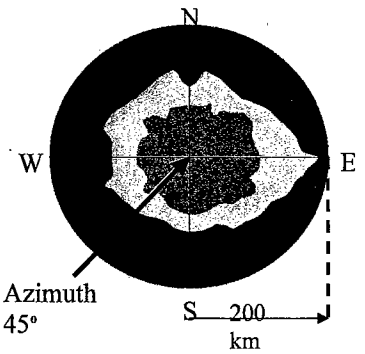

Fig. 4. Azimuthal performance view of spherical Rytov, based on C_n^2 values at the midlevel altitude between target and laser weapon system. The target is at the center.

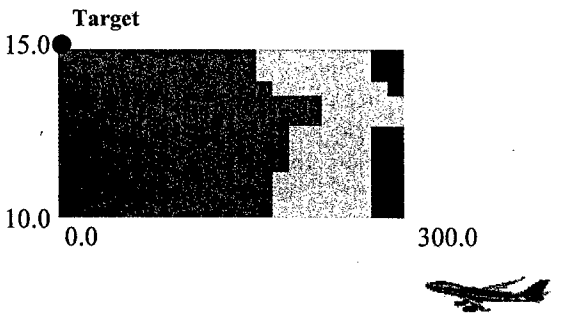

Fig. 5. Example of a vertical cross section of spherical Rytov variance. The unit for both altitude and range is kilometers. The target is located in the upper-right-hand corner of the rectangle. The weapon system can be anywhere in the rectangle.

in green, moderate values in yellow, and the greatest values in red. The user supplies the spherical Rytov thresholds that define each color level. From this view, the user can see whether there is clearly a better azimuth for the orbit of the system. These results are only an approximation of the values that will be computed later, since the C_n^2 values for the azimuthal view are those of the midlevel altitude between target and laser weapon system.

Once an azimuth is selected, the next question is the best distance to orbit from the target watchbox. Generally the greater the distance, the better for the safety and flexibility of the laser crew; yet the performance of the laser generally decreases with range. To assist in the range decision, DEEST provides a cross-section view between the user-selected position of the laser and the target, which are shown on the map in Figs. 3 and 6. Numerical values of this information are also shown in the tables to the right of the map. An example cross section is shown in Fig. 5, which shows colored contours of spherical Rytov values. The section shown is for altitudes of 10.0–15.0 km and ground ranges of 0.0–300.0 km from the enemy missile in the direction of the laser system. In a vertical cross section, the enemy missile is always located on the y axis at a vertical extreme. If the enemy missile has altitude greater than that of the laser system, the enemy missile is located in the upper-left-hand corner of the vertical cross section. If the enemy missile has altitude lower than that of the laser system, then the enemy missile is located in the lower-left-hand corner of the vertical

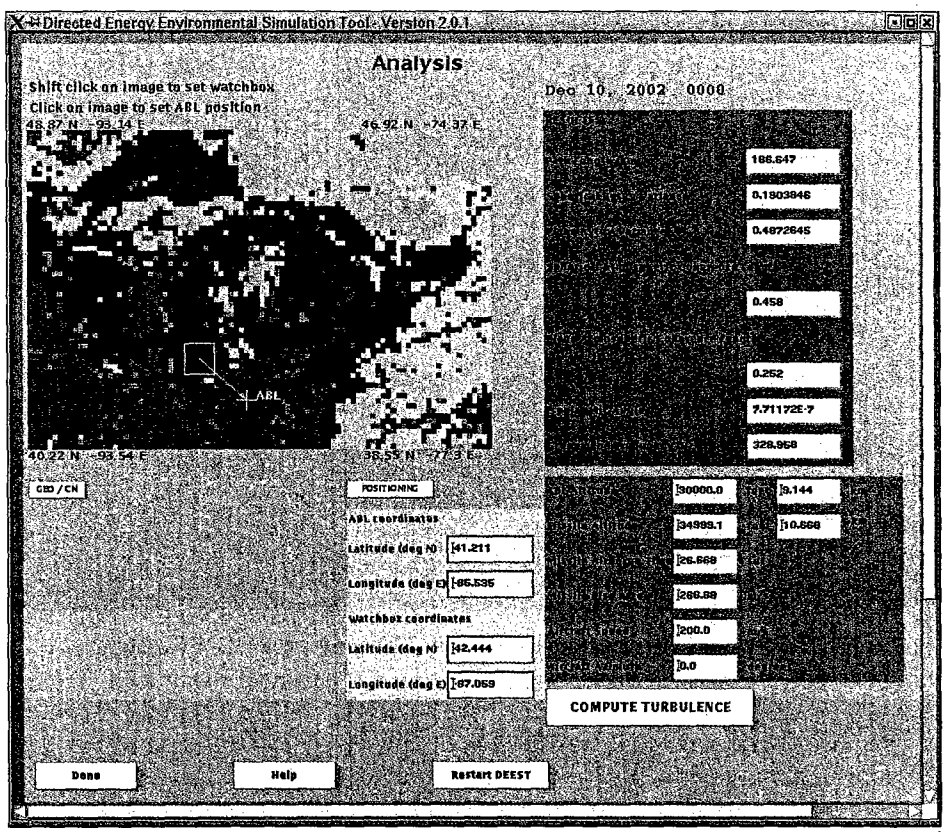

Fig. 6. DEEST GUI analysis screen (wavelength = 1.315 μm).

cross section. Spherical Rytov values are computed for all ground ranges and altitudes to construct the vertical cross-section image. From this cross section, one can judge what is the best distance for the laser orbit, given its flight altitude.

Once the user has set up the general scenario from the planning page, the analysis page is used for more precise performance estimates. The page consists of a map and numerical information as shown in Fig. 6.

There are many user options as to how and which results are to be displayed. The user can toggle the background image between geographic and C_n^2 background images by clicking on the GEO/CN button. The integration boundaries for C_n^2 and clouds can be altered with the base height and top height text fields. The weighting coefficients for the cloud calculation can be changed to adjust the relative influences of liquid, ice, rain, and snow on cloud opacity.

For Greenwood frequency computations, note that the user can enter laser aircraft speed. The positions of the system and target can be changed by using numerical or graphical input. Results are recalculated to reflect new positions. The target (missile) speed will be a function of altitude.

A different selection of images is used to show turbulence and cloud predictions produced by a "ground-to-space" version of DEEST. Figure 7 shows a C_n^2 image for the entire CONUS region. This image contains vertical column integrals of C_n^2 from 0.4 to 22.0 km above

Fig. 7. Vertical integrated C_n^2 from 0.4 to 22 km over the CONUS region.

Fig. 8. Vertical integrated C_n^2 and cloud obscuration over the CONUS region.

ground level. The image color is scaled two standard deviations about its mean value: black is the minimum, white is the maximum, and the mean is bright yellow. This image is for October 12, 2002, at 1500 GMT.

If the user selects that clouds be shown, the opaque clouds are shown in gray on a C_n^2 image, as shown in Fig. 8. Once the integral for the cloud water mixing ratio reaches a

threshold value over the vertical ray for a given grid cell, the grid cell is considered opaque to optical turbulence and a gray grid cell (i.e., a cloud-filled grid cell) is portrayed on the image.

It is important to keep in mind that these C_n^2 values are computed from numerical model data. Obviously, thermosondes can measure finer-scale C_n^2 features in the vertical than can be represented by mesoscale-modeled data. Measured, fine-scale C_n^2 data have high spatial and temporal variance, whereas a model will filter and smooth observed meteorological data and the postprocessed C_n^2 values. The goal of the model data is to estimate the performance integrals of the model as close as possible to the results from the measured data. Computing C_n^2 values from smoothed data can go only so far in simulating observed C_n^2 measurements in the atmosphere.

9. Verification

One use of DEEST is to assist in the validation of the C_n^2 parameterizations that are used in the model. In developing DEEST, a considerable amount of time was spent verifying that the DEEST computed C_n^2 values were the same as those computed with earlier FORTRAN postprocessors used to compute C_n^2 and the performance integrals from MM5 output. The forecast turbulence from MM5 and the Dewan model is routinely compared to measured C_n^2 values using the thermosonde.[23] In addition, "perfect-prog" methods are used for verification, where thermosonde C_n^2 measurements are compared to the Dewan model, using as input the temperature, pressure, and wind velocity measured by the radiosonde attached to the thermosonde. Current verification efforts have concentrated on improving the lower-altitude turbulence models by using thermosonde data and optical measurements from the generalized scidar,[15] a telescope-mounted, remote sensor to locate and measure regions of optical turbulence.

10. Summary and Conclusions

The primary atmospheric phenomena affecting laser transmission are optical turbulence, clouds, aerosols, atmospheric molecular absorption, path refraction, and thermal blooming. The actual ranking of impacts is strongly influenced by scenario details such as altitude, location, target and laser weapon velocity, season, and even time of day. The scale of the simulation will largely dictate the required dimensional fidelity (one dimensional, three dimensional, layered, onion skin, etc.). The Air Force Research Laboratory has used either one-dimensional onion-skin models based on the historical thermosonde database or three-dimensional models based on mesoscale model output, either operational or research grade, and parameterizations of the important atmospheric impacts that are not explicitly computed by the mesoscale model.

The Directed Energy Environmental Simulation Tool (DEEST) is a software tool for optical turbulence calculations depicting atmospheric engagements between a laser system vehicle and an enemy missile. DEEST accomplishes optical turbulence modeling with five models, and to date, calculations have been driven from operation mesoscale model forecast data supplied by AFWA.

The user interface that drives DEEST is designed with mission planning purposes in mind, but it could be useful for other modeling and simulation efforts. In particular, the user either graphically or numerically defines the laser paths of interest in terms of the system and target positions. The DEEST user can create horizontal and vertical cross-sectional views of

egion.

S region.

an value: black
is image is for

n gray on a C_n^2
ratio reaches a

spherical wave Rytov variance to help determine the angle from which to approach and aim at a target missile. Once positional planning is established, the user can obtain precise path-integrated optical performance parameters for C_n^2-derived parameters along the beam path. These calculations include opaque cloud representation by considering a grid cell to be cloud filled once a summation of weighted water specie mixing ratios exceeds a threshold value.

The models currently included in DEEST address atmospheric regions of interest to airborne, ship-based, and ground-based systems. It has been demonstrated that DEEST can operate as a Web-based tool with periodically updated optical parameter quantities for a limited domain, such as a theater of potential military activity with operational weather data.

11. Acknowledgments

DEEST was originally assembled with funding from the Air and Space Modeling and Simulation Executive Agent, as an extension of the Hyper-Cube concept. The Office of the Secretary of Defense High Energy Laser Joint Technology Office sponsored additional work on DEEST. They also sponsored much of the analysis of the onion-skin profiles, and the recent improvements to the HITRAN model. We also acknowledge the mesoscale meteorological forecasts generated by the Air Force Weather Agency. The Air Force Research Laboratory, under the guidance and support of the Battlespace Surveillance Innovation Center Branch Chief, Dr. Robert R. Beland, funded the remainder of the effort.

References

[1]Adair, S., G. Fairley, G. Seeley, and G. Jumper, *The Directed Energy Environmental Simulation Tool: Features and Philosophy*, The Battlespace Atmospheric and Cloud Impacts on Military Operations (BACIMO) Conference, September 9–11, 2003, Monterey, CA (2003) <http://www.nrlmry.navy.mil/bacimo2003/proceedings/P2-03Adair.doc>.

[2]Beland, R.R., *The Infrared and Electro-Optical System Handbook. 2, Atmospheric Propagation of Radiation*, edited by F.G. Smith, Infrared Information Analysis Center, Ann Arbor, MI, and SPIE Engineering Press, Bellingham, WA, pp. 157–232 (1993).

[3]Businger, S., R. McLaren, R. Ogasawara, D. Simons, and R.J. Wainscoat, Bull. Amer. Meteorol. Soc. June, 858 (2002).

[4]Dewan, E.M., R.E. Good, R. Beland, and J. Brown, "A Model for C_n^2 (Optical Turbulence) Profiles Using Radiosonde Data," Phillips Laboratory Technical Report PL-TR-932043. ADA 279399 (1993).

[5]Doss-Hammel, S.M., D. Tsintikidis, A.M.J. van Eijk, and G.J. Kunz, "Prediction and Exploitation: The Use of the EOSTAR Model in the Marine Infrared Propagation Environment," The Battlespace Atmospheric and Cloud Impacts on Military Operations (BACIMO) Conference, September 9–11, 2003, Monterey, CA (2003) <http://www.nrlmry.navy.mil/bacimo2003/proceedings/P2-09 Doss-Hammel.pdf>.

[6]Dudhia, J., "MM5 Dynamics and Numerics," University Corporation for Atmospheric Research (UCAR) [Webpage] [Jan. 2003]; <http://www.mmm.ucar.edu/mm5/mm5v3/tutorial/presentations/MM5_eq/img26.html> [Accessed 24 July 2003].

[7]Dudhia, J., Monthly Weather Rev. **121**, 1493 (1993).

[8]Dudhia, J., D. Gill, Y.-R. Guo, D. Hansen, K. Manning, and W. Wang, "PSU/NCAR Mesoscale Modeling System Tutorial Class Notes and Users' Guide (MM5 Modeling System Version 3)," University Corporation for Atmospheric Research (UCAR) [Web page][Jan. 2003]; <http://www.mmm.ucar.edu/mm5/documents/> [Accessed 24 July 2003].

[9]Frederickson, P.A., K.L. Davidson, and C.S., Bendall, J. Appl. Meteorol. **39**, 1770 (2000).

[10]Greenwood, D., J. Opt. Soc. Am. **67**(3), 390 (1977).

[11]Grell, G.A., J. Dudhia, and D.R. Stauffer, *A Description of the Fifth Generation Penn State/NCAR Mesoscale Model (MM5)*, p. 112 (1994).

[12]Grell, G., J. Dudhia, and D. Stauffer, "A Description of the Fifth-Generation Penn State/NCAR Mesoscale Model (MM5)," University Corporation for Atmospheric Research (UCAR) [Webpage][Jan. 2003]; <http://www.mmm.ucar.edu/mm5/documents/> [Accessed 24 July 2003].

[13]HITRAN, the HITRAN Database Web site; <http://cfa-www.harvard.edu/HITRAN/> [accessed 9 March 2005].

[14]Holton, J.R., *An Introduction to Dynamic Meteorology*, Academic Press, pp. 124–125 (1992).

[15]Jumper, G.Y., E.A. Murphy, A.J. Ratkowski, and J. Vernin, "Multi-Sensor Campaign to Correlate Atmospheric Optical Turbulence to Gravity Waves," AIAA Paper 2004-1077 (2004).

[16]Kaimal, J.C., J.C. Wyngaard, D.A. Haugen, O.R. Cote, and Y. Izumi, J. Atmos. Sci. **33**, 2152 (1976).

[17]Miller, D., and D. Walters, 2003, "Mesoscale Model Forecasts of Optical Turbulence: Lessons Learned and New Refinements," The Battlespace Atmospheric and Cloud Impacts on Military Operations (BACIMO) Conference, September 9–11; 2003, Monterey, CA (2003) <http://www.nrlmry.navy.mil/bacimo2003/presentations/)P7-09Miller.doc>.

[18]Rachele, H., and A.D. Tunick, J. Appl. Meteorol. **34**, 964 (1994).

[19]Roadcap, J.R., P.J. McNicholl, and R.R. Beland, *Analysis of Thermosonde Data for High Energy Laser Tactical Applications*, The Battlespace Atmospheric and Cloud Impacts on Military Operations (BACIMO) Conference, September 9–11, 2003, Monterey, CA (2003) <http://www.nrlmry.navy.mil/bacimo2003/proceedings/P2-04 Roadcap.doc>.

[20]Roadcap, J.R., P.J. McNicholl, R.R. Beland, and G.Y. Jumper, "Estimates of Atmospheric Distortion Number for Non-linear Refraction," *Proceedings, Second Directed Energy Modeling & Simulation Conference*, 9–11 March 2004, Huntsville, AL (2004).

[21]Rogers, R.R., and M.K. Yau, *A Short Course in Cloud Physics*, Pergamon Publications, 3rd ed. (1989).

[22]Rothman, L.S., R.R. Gamache, R.H. Tipping, C.P. Rinsland, M.A.H. Smith, D.C. Benner, V. Malathy Devi, J.M. Flaud, C. Camy-Peyret, A. Perrin, A. Goldman, S.T. Massie, L.R. Brown, and R.A. Toth, J. Quant. Spectrosc. Radiat. Transfer **48**, 469 (1992).

[23]Ruggiero, F.H., and D.A. DeBenedictis, Forecasting optical turbulence from mesoscale numerical weather prediction models. Preprints, HPCMP Users Group Conference 2002, 10–14 June, Austin, TX (2002) <http://www.hpcmo.hpc.mil/Htdocs/UGC/UGC02/paper/frank_ruggiero1_paper.pdf>.

[24]Swanson, R.T., M.D. McAtee, and R.L. Ritz, "Operational Mesoscale Data Assimilation at Air Force Weather Agency Using a Parallelized Multivariate Optimal Interpolation Scheme," The Eleventh PSU/NCAR Mesoscale Model Users' Workshop, Boulder, CO, pp. 27–29 (2001).

[25]Tatarski, V.I., *Wave Propagation in a Turbulent Medium*, McGraw–Hill, pp. 55–58 (1961).

[26]Tunick, A.D., "The Refractive Index Structure Parameter/Atmospheric Optical Turbulence Model: CN2," U.S. Army Research Laboratory. ARL-TR-1615 (1998).

[27]Tunick, A.D., "Calculating the Microstructure of Atmospheric Optical Turbulence: CN2," U.S. Army Research Laboratory Report (1998).

[28]University Corporation for Atmospheric Research (UCAR) [Web page][May 2000]; <http://deved.comet.ucar.edu/nwp/pcu2/afassim1.htm> [Accessed 24 July 2003].

[29]University Corporation for Atmospheric Research (UCAR) [Web page][May 2000]; <http://deved.comet.ucar.edu/nwp/pcu2/afassim3.htm> [Accessed 24 July 2003].

[30]University Corporation for Atmospheric Research (UCAR) [Web page][May 2000]; <http://deved.comet.ucar.edu/nwp/pcu2/afhres2.htm> [Accessed 24 July 2003].

[31]University Corporation for Atmospheric Research (UCAR) [Web page][May 2000]; <http://www.mmm.ucar.edu/mm5/documents/mm5-code-pdf/sec1.pdf> [Accessed 24 July 2003].